

were made from the oligonucleotide positive retina, in which most RGCs showed strong fluorescence.

Electrophysiology and visual stimulation

Whole-cell perforated recording from RGCs or tectal cells were made under visual control by methods described previously²⁸. The micropipettes were made from borosilicate glass capillaries (Kimax), had a resistance in the range of 2–3 MΩ, and were tip-filled with internal solution and then were back-filled with internal solution containing 200 μg ml⁻¹ amphotericin B. The internal solution contained: 115 mM K-gluconate, 4 mM NaCl, 1.5 mM MgCl₂, 20 mM HEPES at pH 7.3 and 0.5 mM EGTA. Recordings were made with a patch clamp amplifier (Axopatch 200A; Axon Instruments). The whole cell capacitance was fully compensated and the series resistance (10–20 MΩ) was compensated at 75–80% (lag 60 μs) and monitored during the experiment. The data were discarded if the series resistance varied by >20%. The input resistance of RGCs at –60 to –70 mV was usually in the range of 0.5 to 1 GΩ. Signals were filtered at 5 kHz and sampled at 10 kHz using Axoscope software (Axon Instruments). For cell-attached recording, the pipette was filled with bath solution and a loose seal was made. To record mEPSCs from RGCs or tectal neurons, TTX (1 μM) was added to external solution. A total amount of 400 ng BDNF (PeproTech), dissolved in 15 μl bath solution containing 0.1% bovine serum albumin (BSA), was puffed into the third ventricle near the tectum through a Picospritzer II (General Valve), using a micropipette with a tip opening of 6 μm and repetitive pressure pulses (5 psi, 0.5 Hz, 1 s duration). It usually took 15 min for the BDNF-containing solution to be completely ejected. A small LCD-screen (Sony, PLM-A35) was mounted on the camera port of the microscope, allowing projection of computer-generated images onto the retina of the tadpole. Light responses were evoked by whole-field stimulations with a step (4 s) increase in the whole-field light illumination. All drugs were from Sigma.

Data analysis

Mini analysis (6.0.1 from Synaptosoft) was used to detect and analyse mEPSCs, sEPSCs and spikes, and the same program was used for peak-scaled non-stationary noise analysis of mEPSCs or sEPSCs, using the method previously described^{29,30}. The relationship between the variance (σ^2) and the amplitude (I) of mEPSCs or sEPSCs was fitted by the parabola $\sigma^2 = i \times I - I^2/N$, where the estimated weighted single-channel current (i) and the mean receptor number per synapse (N) were derived from the best fit. The estimated weighted single-channel conductance (g_s), was derived from the relationship: $g_s = i / (E_{rev} - V_c)$, where E_{rev} is the reversal potential of EPSCs, and V_c the holding potential. The mean channel open probability of synaptic receptors (p_o), was calculated by the function: $p_o = I_m / (i \times N)$, where I_m is the amplitude of mean mEPSCs or sEPSCs. A prerequisite of applying the noise analysis is that data are not filtered by the recording system and electrotonic structure of the cell (see Supplementary Methods). Statistical analysis was performed using paired Student's t -test and summary data are presented as means \pm s.e.m.

Received 17 December 2003; accepted 7 May 2004; doi:10.1038/nature02618.

1. Fitzsimonds, R. M., Song, H. J. & Poo, M. M. Propagation of activity-dependent synaptic depression in simple neural networks. *Nature* **388**, 439–448 (1997).
2. Tao, H. W., Zhang, L. I., Bi, G. Q. & Poo, M. M. Selective presynaptic propagation of long-term potentiation in defined neural networks. *J. Neurosci.* **20**, 3233–3243 (2000).
3. Rumelhart, D. E., Hinton, G. E. & Williams, R. J. Learning representations by back-propagation errors. *Nature* **323**, 533–536 (1986).
4. Cohen-cory, S. & Fraser, S. E. BDNF in the development of the visual system of *Xenopus*. *Neuron* **12**, 747–761 (1994).
5. Huang, E. J. & Reichardt, L. F. Neurotrophins: roles in neuronal development and function. *Annu. Rev. Neurosci.* **24**, 677–736 (2001).
6. Lohof, A. M. & Poo, M. M. Potentiation of developing neuromuscular synapses by the neurotrophins NT3 and BDNF. *Nature* **363**, 350–353 (1993).
7. Lessmann, V., Gottmann, K. & Heumann, R. BDNF and NT-4/5 enhance glutamatergic synaptic transmission in cultured hippocampal neurons. *Neuroreport* **6**, 21–25 (1994).
8. Li, Y. X. *et al.* Expression of a dominant negative TrkB receptor, T1, reveals a requirement for presynaptic signaling in BDNF-induced synaptic potentiation in cultured hippocampal neurons. *Proc. Natl Acad. Sci. USA* **95**, 10884–10889 (1998).
9. Schinder, A. F., Berninger, B. & Poo, M. M. Postsynaptic target specificity of neurotrophin-induced presynaptic potentiation. *Neuron* **25**, 151–163 (2000).
10. Poo, M. M. Neurotrophins as synaptic modulators. *Nature Rev. Neurosci.* **2**, 24–32 (2001).
11. Isaac, J. T., Nicoll, R. A. & Malenka, R. C. Evidence for silent synapses: implications for the expression of LTP. *Neuron* **15**, 427–434 (1995).
12. Durand, G. M., Kovalchuk, Y. & Konnerth, A. Long-term potentiation and functional synapse induction in developing hippocampus. *Nature* **381**, 71–75 (1996).
13. Wu, G. Y., Malinow, R. & Cline, H. T. Maturation of a central glutamatergic synapse. *Science* **274**, 972–976 (1996).
14. Watson, F. L. *et al.* Rapid nuclear responses to target-derived neurotrophins require retrograde transport of ligand-receptor complex. *J. Neurosci.* **19**, 7889–7900 (1999).
15. von Bartheld, C. S., Byers, M. R., Williams, R. & Bothwell, M. Anterograde transport of neurotrophins and axodendritic transfer in the developing visual system. *Nature* **379**, 830–833 (1996).
16. Ginty, D. D. & Segal, R. A. Retrograde neurotrophin signaling: Trk-ing along the axon. *Curr. Opin. Neurobiol.* **12**, 268–274 (2002).
17. Purves, D. Functional and structural changes in mammalian sympathetic neurons following interruption of their axons. *J. Physiol. (Lond.)* **252**, 429–463 (1975).
18. Purves, D. Effects of nerve growth factor on synaptic depression after axotomy. *Nature* **260**, 535–536 (1976).
19. Wong, W. T., Faulkner-Jones, B. E., Sanes, J. R. & Wong, R. O. Rapid dendritic remodeling in the developing retina: dependence on neurotransmission and reciprocal regulation by Rac and Rho. *J. Neurosci.* **20**, 5024–5036 (2000).

20. Lom, B., Cogen, J., Sanchez, A. L., Vu, T. & Cohen-cory, S. Local and target-derived brain-derived neurotrophic factor exert opposing effects on the dendritic arborization of retinal ganglion cells *in vivo*. *J. Neurosci.* **22**, 7639–7649 (2002).
21. Hartmann, M., Heumann, R. & Lessmann, V. Synaptic secretion of BDNF after high-frequency stimulation of glutamatergic synapses. *EMBO J.* **20**, 5887–5897 (2001).
22. Balkowiec, A. & Katz, D. M. Cellular mechanisms regulating activity-dependent release of native brain-derived neurotrophic factor from hippocampal neurons. *J. Neurosci.* **22**, 10399–10407 (2002).
23. Chytrova, G. & Johnson, J. E. Spontaneous retinal activity modulates BDNF trafficking in the developing chick visual system. *Mol. Cell. Neurosci.* **25**, 549–557 (2004).
24. Constantine-Paton, M., Cline, H. T. & Debski, E. Patterned activity, synaptic convergence, and the NMDA receptor in developing visual pathways. *Annu. Rev. Neurosci.* **13**, 129–154 (1990).
25. Wingate, R. J. & Thompson, I. D. Targeting and activity-related dendritic modification in mammalian retinal ganglion cells. *J. Neurosci.* **14**, 6621–6637 (1994).
26. Churchland, P. S. & Sejnowski, T. J. *The Computational Brain* (MIT Press, Cambridge, Massachusetts, 1992).
27. Nieuwkoop, P. D. & Faber, J. *Normal table of Xenopus laevis*, 2nd edn (North Holland, Amsterdam, 1967).
28. Zhang, L. I., Tao, H. W., Holt, C. E., Harris, W. A. & Poo, M. M. A critical window for cooperation and competition among developing retinotectal synapses. *Nature* **395**, 37–44 (1998).
29. Traynelis, S. F., Silver, R. A. & Cull-Candy, S. G. Estimated conductance of glutamate receptor channels activated during EPSCs at the cerebellar mossy fiber-granule cell synapse. *Neuron* **11**, 279–289 (1993).
30. Benke, T. A., Lüthi, A., Isaac, J. T. R. & Collingridge, G. L. Modulation of AMPA receptor unitary conductance by synaptic activity. *Nature* **393**, 793–797 (1998).

Supplementary Information accompanies the paper on www.nature.com/nature.

Acknowledgements We thank X. H. Zhang for writing the software of light stimulation and Z. R. Wang for establishing the method of TrkB knockdown of *Xenopus* tadpoles. This work was supported by grants from the NIH.

Competing interests statement The authors declare that they have no competing financial interests.

Correspondence and requests for materials should be addressed to M.M.P. (mpoo@uclink.berkeley.edu).

Gene regulation and DNA damage in the ageing human brain

Tao Lu¹, Ying Pan¹, Shyan-Yuan Kao¹, Cheng Li², Isaac Kohane³, Jennifer Chan⁴ & Bruce A. Yankner¹

¹Department of Neurology and Division of Neuroscience, The Children's Hospital and Harvard Medical School, Enders 260, 300 Longwood Avenue, Boston, Massachusetts 02115, USA

²Department of Biostatistics, Harvard School of Public Health, and ³Department of Medicine, The Children's Hospital and Harvard Medical School, and

⁴Department of Pathology, Brigham and Women's Hospital and Harvard Medical School, Boston, Massachusetts 02115, USA

The ageing of the human brain is a cause of cognitive decline in the elderly and the major risk factor for Alzheimer's disease¹. The time in life when brain ageing begins is undefined^{2–4}. Here we show that transcriptional profiling of the human frontal cortex from individuals ranging from 26 to 106 years of age defines a set of genes with reduced expression after age 40. These genes play central roles in synaptic plasticity, vesicular transport and mitochondrial function. This is followed by induction of stress response, antioxidant and DNA repair genes. DNA damage is markedly increased in the promoters of genes with reduced expression in the aged cortex. Moreover, these gene promoters are selectively damaged by oxidative stress in cultured human neurons, and show reduced base-excision DNA repair. Thus, DNA damage may reduce the expression of selectively vulnerable genes involved in learning, memory and neuronal survival, initiating a programme of brain ageing that starts early in adult life.

To investigate age-dependent regulation of gene expression in the human brain, RNA was harvested from postmortem samples of the

frontal pole of 30 individuals ranging in age from 26 to 106 and was analysed using Affymetrix gene chips. To resolve genes with similar age-dependent expression patterns, the data were analysed for genes that correlate significantly with age and visualized by hierarchical clustering. This analysis demonstrated a cluster of co-regulated genes with reduced expression, and another cluster of genes with increased expression in aged individuals (Fig. 1a). To assess the rate of these gene changes, the entire transcriptome profile was compared at each age, and Pearson correlation coefficients were derived as a measure of similarity between any two ages (Fig. 1b). The group of individuals ≤ 42 years old showed the most homogeneous pattern of gene expression, and the group ≥ 73 years old was also relatively homogeneous (red colour indicating positive correlation).

Moreover, these two age groups were negatively correlated with each other (blue colour indicating negative correlation). In contrast, the middle age group ranging in age from 45–71 exhibited much greater heterogeneity, with some cases resembling the young group and others resembling the aged group (Fig. 1b). These results suggest that a genetic signature of human cortical ageing may be defined starting in young adult life, and that the rate of age-related change may be heterogeneous among middle age individuals.

Age-related genes were identified by performing statistical group comparison of frontal cortical samples from individuals ≤ 42 and ≥ 73 years old. About 4% of the approximately 11,000 genes analysed were significantly changed (1.5-fold or more, Supplementary Table 2). To validate the microarray data, we compared it with

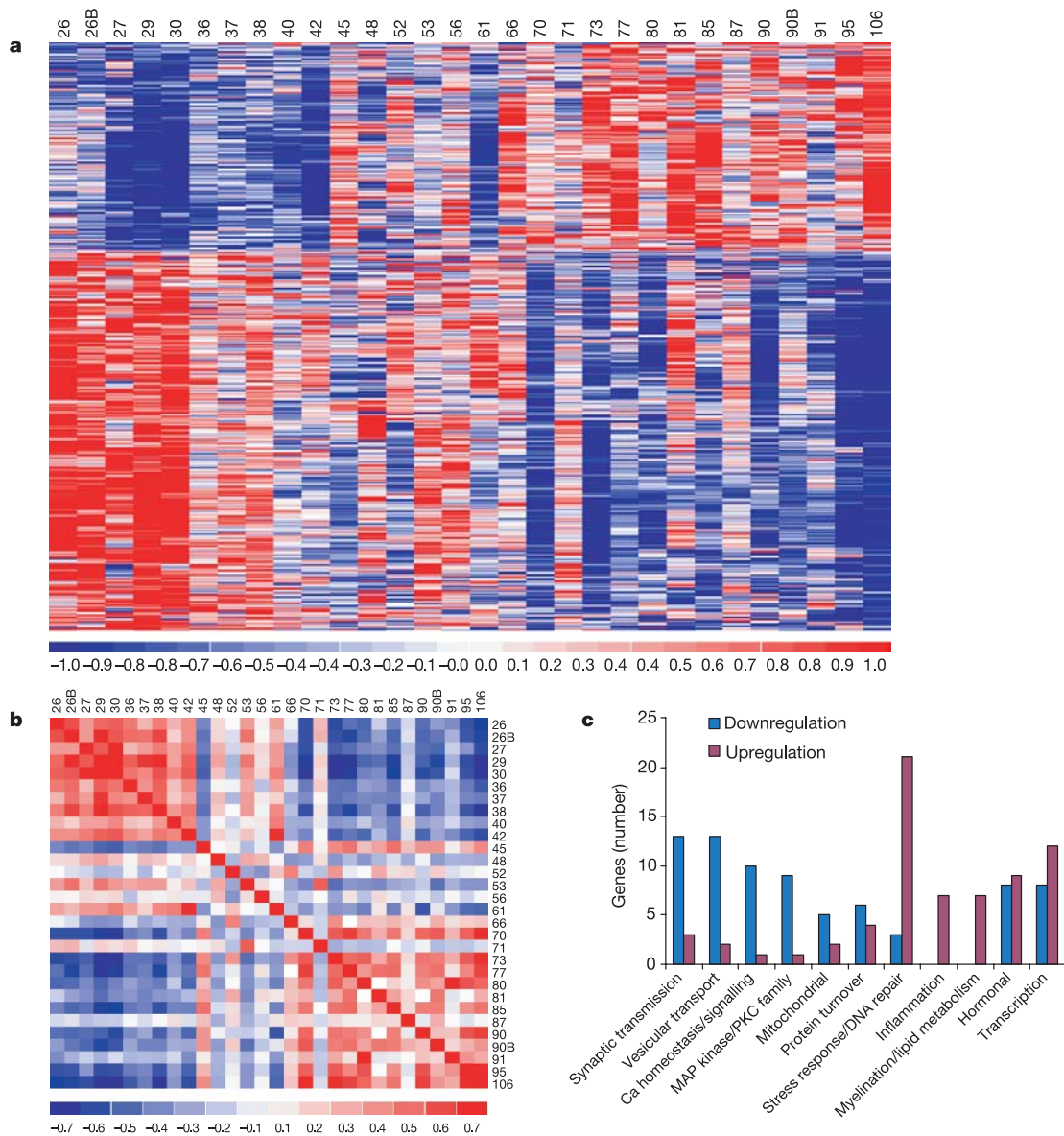


Figure 1 Ageing and gene expression in the human brain. **a**, The transcriptional profile of the normal human prefrontal cortex from 30 individuals ranging in age from 26–106 was analysed by hierarchical clustering of age-regulated genes. One cluster of genes exhibits reduced expression (transition from red to blue), and another cluster exhibits increased expression (transition from blue to red) in aged individuals. Age in years is shown above each lane. Standardized expression values of genes are displayed according to the colour scale, in which red represents above average expression and blue represents below

average expression. Absolute fold changes of individual genes are shown in Table 1 and Supplementary Table 2. **b**, Gene expression profiles were compared between all ages to derive a matrix of Pearson correlation coefficients that indicate the degree of overall similarity between any two cases (see Methods). Positive correlation is indicated by red and negative correlation by blue. Age in years of each case is indicated. The letter B is appended to ages for which there are two independent cases. **c**, Relative changes in gene ontology categories in the aged cortex.

quantitative real-time polymerase chain reaction (PCR) for a subset of functionally important genes. Microarray analysis and quantitative PCR generally showed consistent changes (Fig. 2a). Furthermore, consistent changes at the protein level were observed for a subset of genes analysed by western blotting (Fig. 2b). The post-mortem interval did not correlate significantly with the messenger RNA expression levels of 40 age-regulated genes examined, or with a cumulative measure of all the genes in each of the two age-related clusters (see 'statistical data analysis' in Supplementary Methods). In addition, expression of a number of neuron-specific markers, including β -tubulin, contactin 2 (TAG-1), GAP-43, γ -enolase, and syntaxin 1, did not change significantly with age, suggesting that ageing was not associated with major changes in neuronal cell number.

Genes that play a role in synaptic function and the plasticity that underlies learning and memory were among those most significantly affected in the ageing human cortex (Table 1, Figs 1c and 2). Several neurotransmitter receptors that are centrally involved in synaptic plasticity^{5,6} showed significantly reduced expression after age 40, including the GluR1 AMPA (α -amino-3-hydroxy-5-methyl-4-isoxazole propionic acid) receptor subunit, the NMDA (*N*-methyl-D-aspartate) R2A receptor subunit, and subunits of the GABA_A receptor. Moreover, the expression of genes that mediate synaptic vesicle release and recycling was significantly reduced, notably VAMP1/synaptobrevin, synapsin II, RAB3A and SNAPS.

Members of the major signal transduction systems that mediate long-term potentiation (LTP) and memory storage were age-down-regulated, notably the synaptic calcium signalling system, with reduced expression of calmodulin 1 and CAM kinase II α (Table 1 and Fig. 2a, b). The major calcium-binding proteins calbindins 1 and 2, the calcium pump ATP2B2, and the calcium-activated transcription factor MEF2C that promotes neuronal survival^{7,8}, were also significantly reduced. Furthermore, multiple members of the protein kinase C (PKC) and Ras-MAP (mitogen-activated

protein) kinase signalling pathways showed decreased expression. The activation state of PKC was also reduced, as indicated by decreased levels of activated phosphorylated forms (Fig. 2b). Thus, calcium homeostasis and neuronal signalling may be affected in the aged cortex.

Genes involved in vesicular/protein transport showed reduced expression in the aged cortex, including multiple RAB GTPases, sortilin, dynein, and clathrin light chain (Table 1). Moreover, microtubule-associated proteins (MAP1B, MAP2, tau and kinesin 1B) that stabilize microtubules and promote axonal transport were consistently and robustly reduced. The p35 activator of cyclin-dependent kinase-5 (cdk5), which regulates intraneuronal protein trafficking and synaptic function⁹, was also significantly reduced. Thus, vesicular trafficking may be affected in the aged human cortex. In addition, a number of genes involved in protein turnover also showed reduced expression in aged cortex, including ubiquitin-conjugating enzymes, the lysosomal proton pump, and the enzymes D-aspartate O-methyltransferase and methionine adenosyltransferase II, which repair damaged proteins.

The ageing of the human frontal cortex was also associated with increased expression of genes that mediate stress responses and repair (Fig. 1c and Table 1). These included genes involved in protein folding (heat shock protein 70 and α crystallin), antioxidant defence (nonselenium glutathione peroxidase, paraoxonase and selenoprotein P) and metal ion homeostasis (metallothioneins 1B, 1G and 2A). Genes involved in inflammatory or immune responses, such as tumour-necrosis factor (TNF)- α , were also increased. Increased expression of the base-excision repair enzymes 8-oxoguanine DNA glycosylase and uracil DNA glycosylase is consistent with increased oxidative DNA damage in the aged cortex.

The pronounced downregulation of a defined gene cluster followed by induction of antioxidant and DNA repair genes led us to hypothesize that oxidative DNA damage might target specific genes. Promoter regions may be especially vulnerable, as they contain (G + C)-rich sequences that are highly sensitive to oxidative DNA damage and are not protected by transcription-coupled repair¹⁰. To explore this hypothesis, we devised an assay to detect DNA damage in specific gene sequences. Genomic DNA was isolated under conditions that prevent *in vitro* oxidation, and then cleaved with formamidopyrimidine-DNA glycosylase (FPG), which is an N-glycosidase and AP-lyase that selectively releases damaged bases from DNA, predominantly affecting the major oxidation product 8-oxoguanine¹¹. FPG creates a single-strand break at the apurinic site, rendering it resistant to PCR amplification. Hence, DNA damage to specific sequences can be determined from the ratio of intact PCR products in cleaved versus uncleaved DNA using quantitative PCR. We initially used this assay to assess damage in genomic DNA from fetal human cortex. Fetal cortical DNA did not show significant oxidative DNA damage in the 1-kb upstream promoter regions of several genes that show age-related changes in expression in the adult brain (Fig. 3a).

We then determined whether DNA damage increases in the ageing human cortex, and whether there is a predilection for specific genes. To address this question, we examined the promoters of 30 different genes. Each of these genes showed increased promoter DNA damage in the aged cortex. DNA damage appeared in many genes after age 40, and was most pronounced in all genes after age 70 (Fig. 3b, c). DNA damage also occurred in the exons of these genes with a similar time course, but to a lesser extent than in the promoter regions (data not shown). Biopsy samples of human cortex from individuals who underwent elective neurosurgical procedures showed a similar pattern of age-related DNA damage as postmortem samples (Fig. 3c, asterisks). Thus, DNA damage is pervasive in the ageing human cortex.

We then asked whether gene downregulation in the ageing brain is associated with accelerated DNA damage. To address this question, we determined the increase in promoter DNA damage,

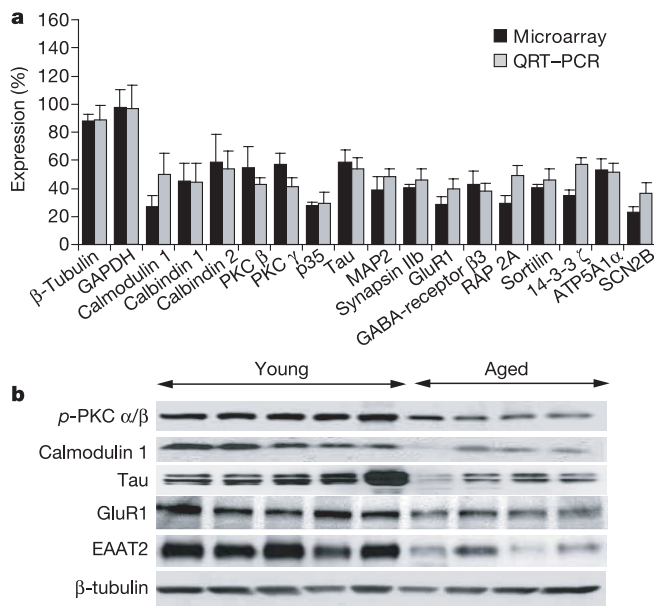


Figure 2 Confirmation of microarray results for synaptic, calcium homeostasis and transport-related genes. **a**, Shown are mRNA levels of selected genes in the aged frontal cortex determined by microarray analysis and quantitative RT-PCR. Values are percentage mRNA levels in aged cases (≥ 73 years old) versus young cases (≤ 42 years old) and represent the mean \pm s.d.; $n = 4$. **b**, Age-related protein levels. Shown are immunoblots from five young and four aged frontal cortical samples. The p-PKC α/β blot specifically resolves activated phosphorylated forms of PKC α/β . EAAT2 is the predominant human brain glutamate transporter.

Table 1 **Age-regulated genes in the human frontal cortex**

Function	Gene name	Accession number	Fold Δ	q value	
Synaptic function					
Synaptic transmission	Glur1	M81886	-2.2 to -2.4	0.002	
	NMDA receptor 2A	U09002	-2.3	0.002	
	GABA A receptor β 3	M82919	-3.2	0.002	
	GABA A receptor α	AF016917	-1.5	0.002	
	Serotonin receptor 2A	AA418537	-2.0	0.002	
	Voltage-gated Na channel II β (SCN2B)	AF049498	-5.1	0.002	
	Voltage-dependent calcium channel β 2	U95019	-1.9	0.002	
	Neurexin 1	AB011150	-1.6	0.002	
	Synaptobrevin 1 (VAMP1)	M36200	-3.4	0.002	
	Synapsin II b	U40215	-3.4	0.002	
	γ -SNAP	U78107	-2.2	0.002	
	α -SNAP	U39412	-1.6	0.005	
	RAB3A	M28210	-1.7	0.002	
	SNAP23	AJ011915	1.7	0.005	
	Synaptophysin-like protein	X68194	1.8	0.006	
	Ca ²⁺ homeostasis/signalling	Calmodulin 1	U12022	-2.2 to -4.1	0.002
		Calmodulin 3	J04046	-1.6	0.002
		Calbindin 1 (28 kD)	AF068862	-2.5	0.002
		Calbindin 2 (29 kD, calretinin)	X56667	-1.6	0.003
		CaM kinase II α	AB023185	-1.7	0.008
CaM kinase IV		D30742	-2.0	0.007	
Calcineurin B α		M30773	-2.8	0.002	
ATPase, Ca ²⁺ -transporting, plasma membrane 2 (ATP2B2)		L20977	-2.5	0.002	
ATPase, Ca ²⁺ -transporting, plasma membrane 2 (ATP2A2)		M23114	-1.6	0.002	
Regucalcin (senescence marker protein)		D31815	1.7	0.002	
Phosphodiesterase 4D		U02882	-1.9	0.002	
Adenylyl cyclase associated protein 2		HG2530	-1.6 to -2.3	0.002-0.003	
Protein kinase C	PKC β 1	X06318	-1.9 to -2.9	0.002	
	PKC γ	Z15114	-1.8	0.002	
G protein signalling	PKC ζ	Z15108	-1.7	0.002	
	Rap2A	X12534	-3.8 to -4.1	0.002	
MAP kinase cascades	Regulator of G protein signalling 4	U27768	-1.8 to -2.2	0.002	
	G protein, q polypeptide (GNAQ)	U43083	-2.0	0.002	
	MAPK1	Z11695	-1.9	0.002	
	MAPK9	U09759	-1.7	0.003	
	MAPKK4	U17743	-3.1	0.002	
	Ras-GNRF	HG2510	-2.4 to -4.7	0.003-0.008	
	MAPKK5	U67156	1.6	0.002	
CdK5	14-3-3 ζ	U28964	-3.6	0.002	
	p21 activated protein kinase (PAK1)	U24152	-2.7	0.002	
	Cdk5, regulatory subunit 1 (p35)	X80343	-3.4	0.002	
Vesicular transport					
Microtubule cytoskeleton	RAB1A	M28209	-1.6	0.006	
	RAB3A	M28210	-1.7	0.002	
	RAB5A	M28215	-1.9	0.002	
	RAB6A	M28212	-3.5	0.002	
	Kinesin 1B	AB011163	-2.2	0.002	
	Sortilin 1	X98248	-3.5	0.002	
	Dynein (DNCH1)	H05552	-2.4	0.002	
	Dynamin 1-like	AF000430	-1.6	0.002	
	Trans Golgi network protein 2	AF027516	-2.2	0.002	
	Golgi reassembly stacking protein 2	W26854	-1.7	0.002	
	Phosphatidylinositol transfer protein β	D30037	-2.0	0.002	
	Clathrin, light polypeptide	M20470	-1.6	0.002	
	Kinesin 2	L04733	1.7	0.005	
	VAMP3	H93123	1.5	0.002	
	MAP1B	L06237	-4.9	0.002	
	MAP2	U01828	-2.1 to -4.2	0.002	
	Tau	J03778	-2.3	0.002	
	RAN binding protein 9	AF064606	-1.7	0.005	
	Neuronal survival				
	Neuronal survival	MADS box transcription enhancer factor 2C (MEF2C)	S57212	-2.7	0.002
Inositol polyphosphate-4-phosphatase I		AI955897	-2.0	0.002	
Inositol 1,4,5 trisphosphate 3 kinase A		X54938	-2.5	0.002	
Inositol 1,4,5 trisphosphate 3-kinase B		X57206	1.9	0.002	
Protein turnover					
Protein turnover	ATPase, H ⁺ -transporting, lysosomal V1 subunit H	W27838	-2.5	0.005	
	ATPase, H ⁺ -transporting, lysosomal V1 subunit A	L09235	-1.7	0.007	
	ATPase, H ⁺ -transporting, lysosomal V1 subunit G 2	W26326	-1.5	0.002	
	Ubiquitin conjugating enzyme Ubch5	HG3344	-1.6	0.002	
	Ubiquitin conjugating enzyme E2M	AF075599	-1.6	0.002	
	Ubiquitin carrier protein	M91670	-1.6	0.002	
	Lysosomal associated membrane protein 2	U36336	2.3	0.002	
	Calpastatin (calpain inhibitor)	D16217	1.6	0.007	
	Serine/cysteine proteinase inhibitor	D83174	1.7	0.005	
	Angiotensinogen (serine /cysteine) proteinase Inhibitor A8	K02215	1.6	0.002	
Amino acid modification					
Amino acid modification	Protein-L-isoaspartate (Daspertate) O-methyltransferase	D25547	-2.7	0.002	
	Methionine adenosyltransferase II α	X68836	-2.1	0.002	
	Beta-1,3-galactosyltransferase	Y15062	-1.9	0.002	
	Glutamate decarboxylase 1	M81883	-1.6	0.005	
	Methionine synthase reductase	AF025794	1.6	0.008	

Table 1 – continued

Function	Gene name	Accession number	Fold Δ	q value
Mitochondrial	Transglutaminase 2	M55153	2.8	0.002
	Glycine amidinotransferase	S68805	1.5 to 1.8	0.002
	Lysine hydroxylase 2	U84573	2.4	0.002
	ATP synthase, H ⁺ -transporting, mitochondrial F1α1	D14710	-2.3	0.002
	Mitochondrial ribosomal protein L28	U19796	-1.7	0.002
	Mitochondrial ribosomal protein S12	Y11681	-2.2	0.002
	Cytochrome c synthase	U36787	-1.6	0.002
Stress response	Translocase of inner mitochondrial membrane 17 A	X97544	-2.0	0.002
	Monoamine oxidase A	AA420624	1.6	0.002
	Mitochondrial 3-oxoacyl-Coenzyme A thiolase	D16294	1.5	0.003
	Nonselenium glutathione peroxidase	D14662	1.7	0.002
Antioxidant	Selenoprotein P	Z11793	1.7	0.002
	Paraoxonase 2	AF001601	1.6	0.002
DNA repair	Cystathionine-beta-synthase	L00972	1.6	0.002
	8-oxoguanine DNA glycosylase	U88620	1.6	0.006
	Uracil-DNA glycosylase	Y09008	1.7	0.005
	Topoisomerase I binding protein	U82939	1.6	0.009
	Topoisomerase II β	M27504	-1.7	0.003
Stress	FK506 binding protein 12-rapamycin associated protein 1	L34075	-1.9	0.002
	Heat shock 70 kD protein 2	L26336	1.9 to 2.2	0.005–0.006
	Crystallin, alpha B	AL038340	1.6 to 2.0	0.002–0.003
	Hypoxia inducible factor 1 α (HIF1 α)	U22431	2.0	0.005
	HIF-1 responsive RTP801	AA522530	2.5	0.002
	Transglutaminase 2	M55153	2.8	0.002
	p53 binding protein 2	U58334	1.7	0.002
	Retinoblastoma-associated protein 140	AB029028	1.8	0.007
	Retinoblastoma-like 2 (p130)	X76061	1.6	0.007
	Stress 70 protein chaperone	U04735	-1.8	0.006
Metal ion homeostasis	Metallothionein 1G	J03910	2.2	0.005
	Metallothionein 1B	M13485	1.6	0.002
	Metallothionein 2A	R92331	1.5 to 1.7	0.002
	Haem binding protein 2	W27949	2.0	0.002
	Haemoglobin β	L48215	2.9 to 3.3	0.002
	Hephaestin	AB014598	1.6	0.002
	Inflammation	TNF-α	AF010312	2.7
C type lectin		X96719	2.7	0.003
H factor (complement)-1		M65292	3.2	0.002
Interferon, gamma-inducible protein 16		M63838	2.0	0.005
Interferon regulatory factor 7		U53831	1.9	0.003
Integrin α5		M14648	1.8	0.002
Integrin β1		X07979	1.7	0.002
Myelination/lipid metabolism	Oligodendrocyte lineage transcription factor 2	U48250	1.7	0.002
	Peripheral myelin protein 22	D11428	1.7	0.003
	Proteolipid protein 1	M54927	1.6	0.002
	Fatty acid desaturase 1	AF009767	1.8 to 2.1	0.002
	Apolipoprotein D	J02611	2.1	0.002
	Low density lipoprotein receptor related protein 4	AB011540	2.0	0.002
	Sterol carrier protein 2	U11313	1.6	0.002
	Phospholipase D3	U60644	-1.6	0.002
Transcription	Transcription factor ZHX2	AB020661	2.1	0.002
	NK2 transcription factor	AF019415	1.5 to 1.8	0.005–0.008
	Inhibitor of DNA binding 4 (ID4)	AL022726	2.3	0.002
	Zinc finger protein 238	U38896	-4.6	0.002
	Forkhead box G1A	X74143	-2.0	0.002
	Chromatin remodelling complex (SMARCC2)	D26155	-1.8	0.002
	ETS2	J04102	-1.7	0.002
	E2F transcription factor 4	S75174	-1.6	0.003
Hormonal	Insulin receptor	X02160	1.6	0.004
	Leptin receptor	AW026535	1.7	0.002
	Orexin receptor	AF041245	1.6	0.002
	Vascular endothelial growth factor	AF022375	1.8	0.005
	Secreted frizzled related protein 1	AF056087	1.9	0.009
	FGF receptor 2	M87770	1.6	0.002
	FGF receptor 3	M64347	1.8	0.002
	FGF2 (basic)	J04513	2.1	0.002
	Proenkephalin	J00123	-2.5	0.003
	Somatostatin	AI636761	-1.8 to -2.9	0.002
	Cholecystokinin B receptor	L10822	-2.7	0.002
	Chromogranin B (secretogranin 1)	Y00064	-1.6	0.007
	RevErbA β receptor (NR1D2)	D16815	-2.9	0.003
	GDNF receptor α2	AF002700	-1.6	0.003
	FGF 12	AL119322	-2.4 to -2.6	0.002–0.008
FGF 13	U66198	-2.3 to -3.2	0.002–0.005	

Shown are selected age-regulated genes representative of functional groups. Age-downregulated genes are blue and age-upregulated genes are red. Fold changes and statistical q values with a range reflect multiple probe sets for the same gene. Gene accession numbers are provided. See Supplementary Table 2 for a complete list of age-regulated genes.

indicated by the reduction in intact DNA, in individuals over 70 years old. This index of DNA damage was compared for genes that were downregulated, upregulated or stably expressed in the aged cortex. Stably expressed and upregulated genes showed a narrow range of promoter DNA damage in aged cortex (Fig. 3d). In contrast, most of the age-downregulated genes showed significantly greater DNA damage in the aged cortex ($P < 0.001$) (Fig. 3d). These results were confirmed by independently assaying 8-oxoguanine through cleavage of genomic DNA with the 8-oxoguanine-specific

N-glycosylase human OGG1. 8-oxoguanine levels were markedly increased in the promoters of most of the age-downregulated genes examined (Fig. 3e). Chromatin immunoprecipitation of the calmodulin 1 promoter with a monoclonal antibody to 8-oxoguanine confirmed an approximately eightfold increase in 8-oxoguanine in aged cortical samples (Fig. 3f). Thus, accelerated DNA damage is associated with reduced gene expression in the aged human cortex.

To obtain greater insight into the effects of DNA damage on gene expression, we produced human neuroblastoma SH-SY5Y cell lines

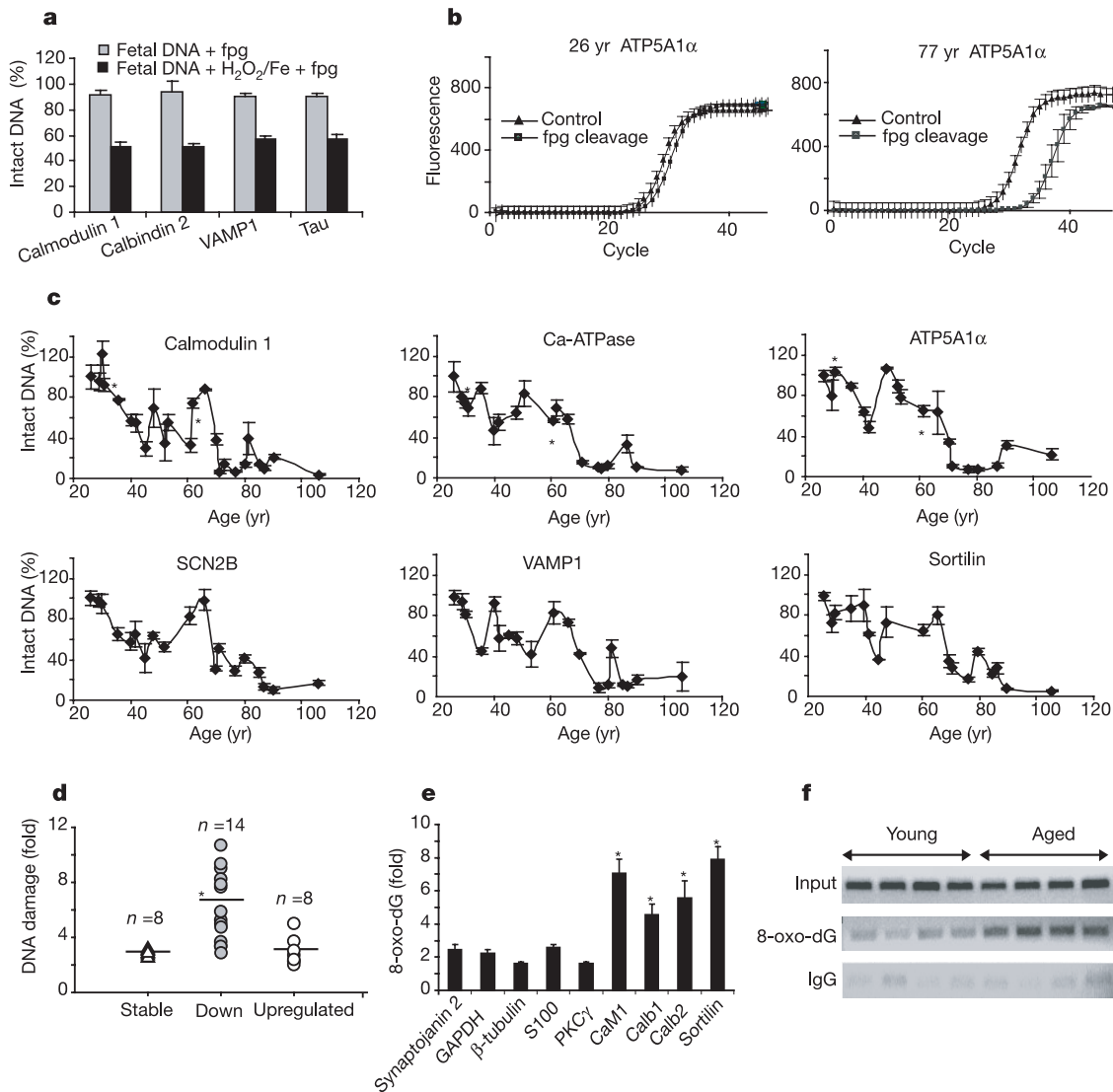


Figure 3 DNA damage in the ageing human cortex. **a**, Genomic DNA from fetal cortex does not exhibit significant DNA damage. DNA damage to the promoter regions of the indicated genes was assayed by cleavage with the endoglycosidase FPG and quantitative PCR. Intact DNA is the percentage detected by PCR following FPG cleavage relative to that in uncleaved DNA. **b**, Ageing increases oxidative DNA damage to the mitochondrial ATP synthase α (ATP5A1 α) promoter. Shown are real-time fluorescence PCR curves from 26- and 77-year-old frontal cortical samples. Note the marked shift in PCR cycle number following FPG cleavage of 77 yr old DNA. Values in **a** and **b** represent the mean \pm s.d. **c**, Time course of DNA damage in the ageing frontal cortex. DNA damage was assayed in the promoters of age-downregulated genes (calmodulin 1, Ca-ATPase, ATP5A1 α , sodium channel $\beta 3$ (SCN2B), VAMP1, and sortilin) in cortical samples from 26- to 106-year-old cases and normalized to the 26-year-old value (100%). Values represent the mean \pm s.d.; $n = 3$. Asterisks indicate intracortical biopsy samples. **d**, DNA damage to

promoters of genes that are stably expressed, downregulated or upregulated in the aged cortex. Shown is the fold increase in promoter DNA damage in aged cases (≥ 70 years old) relative to the youngest, 26-year-old case. Each point represents a gene (see 'DNA damage assay' in Supplementary Methods for gene identities). Asterisk indicates $P < 0.001$ relative to age-stable genes by analysis of variance (ANOVA) with post-hoc Student–Newman–Keuls test. **e**, Oxidative damage to gene promoters in the aged cortex. Shown is the fold increase in 8-oxoguanine (8-oxo-dG) incorporation into promoters of age-stable (GAPDH, β -tubulin and synaptotagmin 2), age-upregulated (S100), and age-downregulated genes (calmodulin 1 (CaM1), calbindin 1 (Calb1), calbindin 2 (Calb2), sortilin and PKC γ). Asterisks indicate $P < 0.05$ relative to GAPDH. Values represent the mean \pm s.e.m.; $n = 4$. **f**, Chromatin immunoprecipitation of the calmodulin 1 promoter with a monoclonal antibody to 8-oxoguanine in aged (≥ 73 -year-old) and young (< 40 -year-old) cortical samples. Input DNA and non-specific IgG (IgG) controls are shown.

that stably overexpress the base-excision repair enzyme human OGG1^{12,13}. Oxidative DNA damage was induced by incubating SH-SY5Y cells with H₂O₂ and FeCl₂, resulting in rapid DNA damage to the promoter of the tau gene, followed by slow and incomplete DNA repair (Fig. 4a). In contrast, human OGG1-overexpressing

SH-SY5Y cells showed augmented DNA repair with complete restoration of intact DNA (Fig. 4a). Tau mRNA expression was also reduced by oxidative stress, but was completely restored by overexpression of human OGG1 (Fig. 4b). Cell viability was not significantly affected by the mild oxidative stress treatment or by

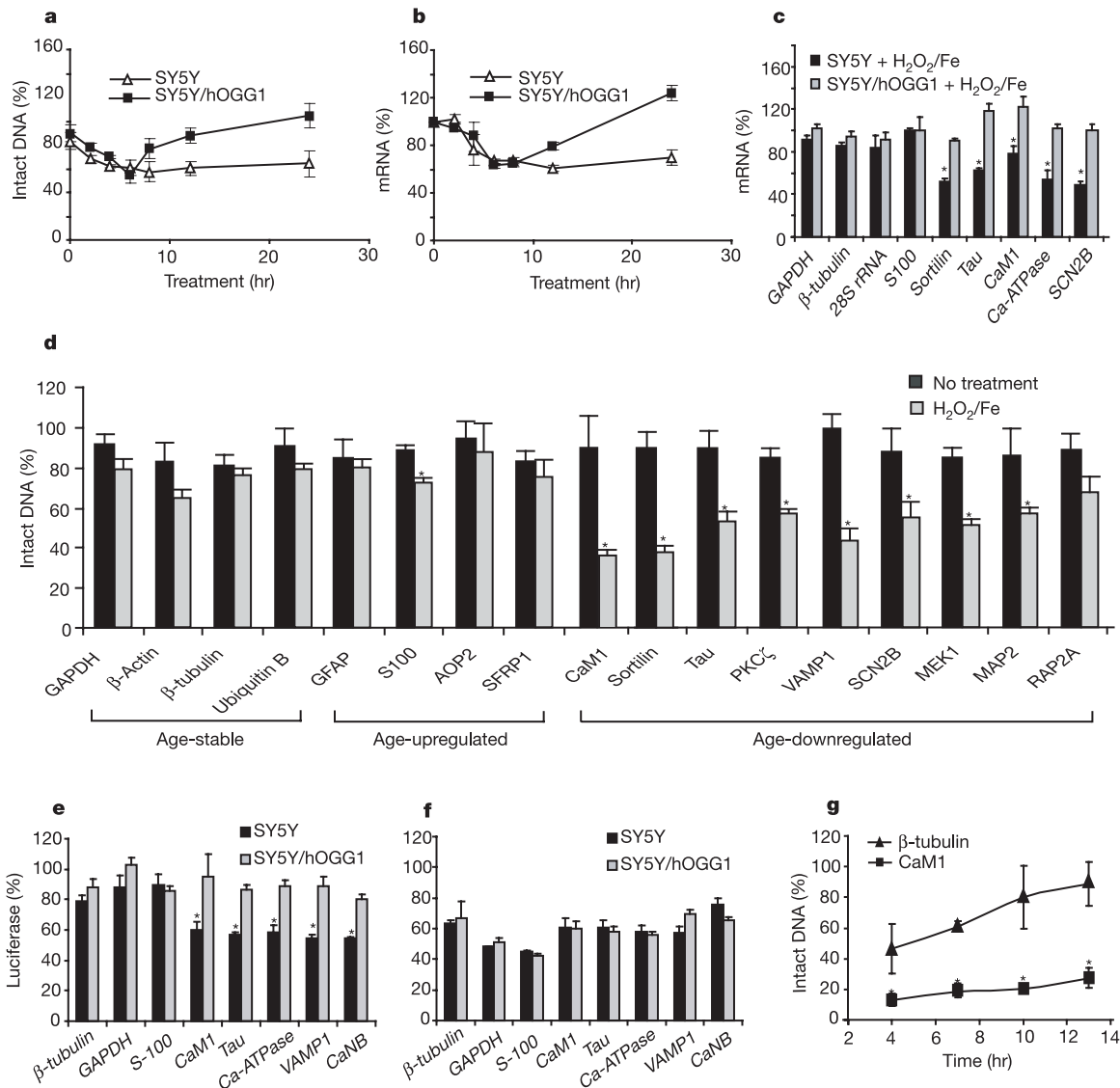


Figure 4 Promoters of age-downregulated genes show increased vulnerability to oxidative DNA damage. **a, b**, Human neuroblastoma SH-SY5Y cells were incubated with H₂O₂/FeCl₂ for the indicated time intervals to induce oxidative DNA damage. DNA damage (**a**) and mRNA expression (**b**) of the tau gene were determined in cells that overexpress the DNA repair enzyme human OGG1 (SY5Y/hOGG1) or the empty pcDNA3 vector (SY5Y). DNA damage was determined by the FPG cleavage/PCR-based assay. Values represent the mean ± s.e.m. **c**, mRNA levels of age-downregulated genes are selectively reduced by oxidative stress and restored by human OGG1. mRNA levels are expressed as percentage in the presence versus absence of H₂O₂/FeCl₂ and represent the mean ± s.e.m.; *n* = 4. Asterisk indicates *P* < 0.05 relative to no treatment by ANOVA with post-hoc Student–Newman–Keuls test. **d**, Increased vulnerability to oxidative DNA damage in promoters of age-downregulated genes. Human cortical neuronal cultures were incubated in the presence or absence of 100 μM H₂O₂/20 μM FeCl₂ for 12 hours and promoter DNA damage was assayed. Values represent the mean ± s.d.; *n* = 3. Asterisks indicate *P* < 0.05 relative to no treatment. *P* < 0.001 for the group of age-downregulated genes relative to age-stable or age-upregulated genes. **e**, Reduced

transcriptional activity of promoters of age-downregulated genes following oxidative DNA damage. Luciferase reporter plasmids derived from the promoters of age-downregulated genes (calmodulin 1 (CaM1), tau, Ca-ATPase, VAMP1/synaptobrevin, and calcineurin B (CaNB)) and genes without reduced expression (β-tubulin, GAPDH and S100) were incubated in the absence or presence of 100 μM H₂O₂ for one hour *in vitro*, and then transfected into SH-SY5Y or SH-SY5Y/human OGG1 cells. Shown is luciferase activity of the damaged reporter expressed as percentage of the activity of the undamaged reporter after 16 h. Values represent the mean ± s.d.; *n* = 4. Asterisk indicates *P* < 0.05 for SH-SY5Y relative to SH-SY5Y/human OGG1. **f**, Ultraviolet damage does not discriminate between promoters of age-stable and age-downregulated genes. Values represent the mean ± s.d. **g**, DNA damage and repair of the β-tubulin and calmodulin 1 (CaM1) promoters. Reporter plasmids damaged *in vitro* by H₂O₂ were transfected and DNA damage was determined within each promoter sequence at increasing time intervals. Values are expressed relative to the transfected undamaged reporter, and represent the mean ± s.d.; *n* = 3. Asterisks indicate *P* < 0.05 relative to β-tubulin.

overexpression of human OGG1 (Supplementary Fig. 1). Thus, oxidative DNA damage can reduce gene expression.

Endogenous mRNA levels of a number of age-downregulated genes (tau, calmodulin 1, Ca-ATPase, sortilin and the sodium channel β) were significantly reduced by mild oxidative stress in SH-SY5Y cells, and restored by human OGG1 (Fig. 4c). In contrast, mRNA levels of genes that are not reduced in the ageing cortex (β -tubulin, GAPDH, S100 and 28S RNA) were not significantly affected (Fig. 4c). Thus, mRNA levels of some age-downregulated genes are highly sensitive to oxidative DNA damage.

We then surveyed a larger number of promoters from age-downregulated and age-stable genes to assess vulnerability to DNA damage in cultured human neurons. After pro-oxidative stress, the promoters of four age-stable and four age-upregulated genes showed minimal declines in the level of intact DNA (Fig. 4d). In contrast, eight of nine age-downregulated promoters showed significantly increased DNA damage. Thus, promoters of age-downregulated genes show increased vulnerability to oxidative DNA damage.

To determine whether reduced DNA repair contributes to promoter vulnerability, we cloned the promoters in luciferase reporter plasmids and performed a host cell reactivation assay¹⁴. Promoter reporter plasmids were damaged *in vitro* by either treatment with H₂O₂ or exposure to ultraviolet light, and then transfected into SH-SY5Y cells, together with an undamaged renilla luciferase control plasmid. Activation of H₂O₂-damaged reporters, an indicator of base-excision repair, was significantly reduced for reporters derived from the promoters of age-downregulated genes relative to reporters derived from age-stable genes (Fig. 4e). Reporter activity was restored by the base-excision repair enzyme human OGG1 (Fig. 4e). In contrast, activation of ultraviolet-damaged reporters was not significantly different for the two promoter categories, and was not affected by human OGG1 (Fig. 4f). Differential promoter damage was confirmed using the FPG cleavage/PCR-based assay. The calmodulin 1 promoter showed more DNA damage than the β -tubulin promoter, and was repaired very slowly (Fig. 4g). In contrast, the β -tubulin promoter was repaired much more rapidly ($P = 0.007$) (Fig. 4g). Thus, both increased initial damage and reduced base-excision repair may contribute to oxidative DNA damage in age-downregulated genes.

One factor that may predispose to DNA damage in the aged cortex is impaired mitochondrial function. Expression of the α subunit of the mitochondrial F1 ATP synthase, which couples oxidative phosphorylation to ATP synthesis, was significantly reduced in the aged human cortex (Table 1 and Fig. 2a). siRNA was used to reduce expression of F1 ATP synthase α mRNA and protein by 2.5-fold in SH-SY5Y cells (Supplementary Fig. 2a,b), approximating the reduction detected in aged human cortex. This resulted in a $24 \pm 1\%$ reduction in cellular ATP levels (mean \pm s.d.; $n = 12$; $P = 0.014$), but did not affect overall cell viability or induce apoptosis. ATP synthase α small interfering RNA significantly increased promoter DNA damage in age-downregulated genes, and reduced mRNA levels (Supplementary Fig. 2c, d). Another siRNA (topoisomerase II β) and random 21-mer oligonucleotide controls had no significant effects (Supplementary Fig. 2a–d). DNA damage induced by knockdown of F1 ATP synthase α was partially reversed by the antioxidant vitamin E (Supplementary Fig. 2c, d). Thus, impaired mitochondrial function can lead to nuclear DNA damage.

Taken together, these findings suggest that accelerated DNA damage may contribute to reduced gene expression in the human brain after age 40. The cluster of age-downregulated genes includes many genes that play integral roles in synaptic plasticity^{5,6}, including NMDA and AMPA receptor function, calcium-mediated signalling, and synaptic vesicle release and recycling. In addition, the reduced expression of key calcium-binding and homeostatic genes in the aged cortex could compromise intraneuronal calcium homeostasis,

as observed in studies of ageing rodent neurons¹⁵, and may increase neuronal vulnerability to toxic insults. Our findings also provide support for the concept of ongoing oxidative stress in the ageing human cortex^{16–18}, as a variety of oxidative stress response and repair genes were induced. Similar stress response genes are induced in the ageing mouse and rat brain^{2–4}, and modulate ageing in *C. elegans*¹⁹. Thus, genome damage may compromise systems that subserve synaptic function and neuronal survival, leading to compensatory stress responses in the aged cortex.

Selective DNA damage to gene promoter sequences is a potential mechanism whereby the expression of specific genes could register the passage of time. Vulnerable DNA sequences appear to show increased initial DNA damage as well as reduced base excision repair. It will be of interest to define the specific vulnerable sequence motifs and their target transcription factors^{20,21}. A previous study showed that there is also substantial oxidative damage to mitochondrial DNA in the ageing human brain²². Our findings suggest that impaired mitochondrial function may contribute to the damage of vulnerable genes in the ageing cortex by increasing reactive oxygen species or by reducing ATP required for DNA repair.

When ageing begins and what triggers its onset is one of the major conundrums of biology. The young adult and extreme aged human populations are relatively homogeneous in their gene expression patterns in prefrontal cortex. However, the middle age population between 40 and 70 years of age exhibits much greater heterogeneity. Thus, individuals may diverge in their rates of ageing as they transit through middle age, approaching a state of 'old age' at different rates. It will be of interest to investigate this relationship in different populations and demographic groups. A recent report suggests that ageing in *C. elegans* and *Drosophila* is characterized by similar changes in orthologous mitochondrial and DNA repair genes, and that the pattern is established in early adulthood²³. Thus, measures to protect the genome early in adult life may influence the rate of subsequent functional decline and the vulnerability of the brain to age-related neurodegenerative diseases. \square

Methods

DNA microarray analysis

Thirty cases spanning ages of 26 to 106 were used for microarray analysis (see Supplementary Information). Dissections of the frontal pole were performed and tissue samples were snap frozen in liquid nitrogen. Total RNA was extracted and complementary RNA targets were prepared, labelled and hybridized with an Affymetrix Test 3 Array. Samples with acceptable RNA quality (see Supplementary Information) were hybridized to Affymetrix HG-U95Av2 oligonucleotide arrays representing about 12,000 probe sets. Three approaches were used to analyse the data. (1) Arrays were normalized and genes that correlated with age (Spearman rank correlation P -value < 0.005) were determined and resolved by hierarchical clustering using dChip V1.3 software (see Supplementary Methods). (2) Correlation coefficient analysis was performed to assess the relatedness of each case to every other case using S-PLUS 2000 software (Insightful Corp.). Gene-wise standardized expression values of the genes that show Spearman rank correlation with age were used to compute Pearson correlation coefficients between two cases. The correlation coefficient matrix containing all pairwise correlation coefficients was then read into dChip for heat-map visualization. The range of observed correlation coefficients was -0.77 to 0.80 , and 0.7 was used as the display range (correlation above 0.7 is pure red, below -0.7 is pure blue, and 0 is white). (3) Significance analysis of microarrays (SAM) software²⁴ was used to compare young (≤ 42 years old) and aged (≥ 73 years old) groups to determine the list of genes with a ≥ 1.5 -fold change and median false discovery rate (FDR) < 0.01 (see Supplementary Tables 2 and 3). Some of the DNA microarray results were validated by quantitative reverse transcription (RT)-PCR and western blot analysis (see Supplementary Methods).

DNA damage analysis

The isolation of genomic DNA for the analysis of oxidative DNA damage was performed under conditions that prevent *in vitro* oxidation, including the presence of $50 \mu\text{M}$ of the free radical spin trap phenyl-tert-butyl nitron (PBN, Sigma), nitrogenation of all buffers, and avoidance of phenol and high temperature (see Supplementary Information). Fetal brain genomic DNA (18 weeks gestation) isolated under these conditions did not show significant oxidative damage (Fig. 3a). DNA damage was assayed by cleavage of genomic DNA with FPG (New England Biolabs), which acts as an efficient N-glycosylase and AP-lyase to excise 8-oxoguanine and other damaged bases, and creates a single-strand break that prevents PCR amplification. Quantitative RT-PCR was then used to determine the content of specific intact sequences. The ratio of PCR products after FPG cleavage to those present in uncleaved DNA was used to determine the percentage of intact DNA.

Incorporation of 8-oxoguanine was assayed by cleavage of genomic DNA with the 8-oxoguanine-specific N-glycosylase human OGG1 (New England Biolabs) and by chromatin immunoprecipitation with a monoclonal antibody to 8-oxoguanine (see Supplementary Methods).

Cell culture

Stable cell lines were derived from human neuroblastoma SH-SY5Y cells by transfection with a pcDNA3.1 vector encoding His-tagged nuclear human OGG1 (a gift from G. Verdine). Stable clonal cell lines were derived by selection in medium containing G418, and human OGG1 expression was confirmed by western blotting. Cells stably expressing the empty pcDNA3.1 vector were used as controls. Human cortical neuronal cultures were established as previously described²⁵. Cells were subjected to a mild pro-oxidative stress by treatment with H₂O₂ and FeCl₂, which did not reduce cell viability during the treatment period (see Supplementary Methods and Supplementary Fig. 1).

Luciferase reporter assays

Gene promoter sequences were identified based on published literature or predictions from the genome data base (see Supplementary Information), PCR-amplified from human brain genomic DNA, and cloned in the luciferase reporter vector pGL3-basic (Promega). The host cell reactivation assay of DNA repair¹⁴ was performed by treating luciferase reporter plasmids with 100 μM H₂O₂ for one hour *in vitro*, or by exposing the DNA to ultraviolet-C light (254 nm) at 200 J m⁻². Damaged or control non-damaged promoter reporter plasmids were transfected into SH-SY5Y or SH-SY5Y/human OGG1 cells together with a pRL-TK-Renilla control plasmid (Promega) using Lipofectamine 2000 (Invitrogen). Sixteen hours after transfection, cells were lysed and analysed by the Dual-Luciferase Reporter Assay (Promega). Reporter luciferase activity was normalized to renilla-luciferase activity to control for transfection efficiency. The luciferase activity of H₂O₂ or ultraviolet-damaged reporters was expressed as the percentage of the luciferase activity of the corresponding non-damaged reporters. To assess DNA damage in the promoter regions of the transfected reporters, the FPG cleavage/PCR-based assay was used with PCR primers against regions of the pGL3 plasmid that encompassed the cloned promoters. This excluded amplification of endogenous promoter sequences of the target genes.

Received 5 March; accepted 14 May 2004; doi:10.1038/nature02661.
Published online 9 June 2004.

1. Yankner, B. A. A century of cognitive decline. *Nature* **404**, 125 (2000).
2. Lee, C.-K., Weindruch, R. & Prolla, T. A. Gene expression profile of the aging brain in mice. *Nature Genet.* **25**, 294–297 (2000).
3. Jiang, C. H., Tsien, J. Z., Schultz, P. G. & Hu, Y. The effects of aging on gene expression in the hypothalamus and cortex of mice. *Proc. Natl Acad. Sci. USA* **98**, 1930–1934 (2001).
4. Blalock, E. M. *et al.* Gene microarrays in hippocampal aging: statistical profiling identifies novel processes correlated with cognitive impairment. *J. Neurosci.* **23**, 3807–3819 (2003).
5. Kandel, E. R. The molecular biology of memory storage: a dialog between genes and synapses. *Science* **294**, 1030–1038 (2001).
6. Malinow, R. & Malenka, R. C. AMPA receptor trafficking and synaptic plasticity. *Annu. Rev. Neurosci.* **25**, 103–126 (2002).
7. Mao, Z., Bonni, A., Xia, F., Nadal-Vicens, M. & Greenberg, M. E. Neuronal activity dependent cell survival mediated by transcription factor MEF2. *Science* **286**, 785–790 (1999).
8. Okamoto, S., Krainc, D., Sherman, K. & Lipton, S. A. Antiapoptotic role of the p38 mitogen-activated protein kinase-myocyte enhancer factor 2 transcription factor pathway during neuronal differentiation. *Proc. Natl Acad. Sci. USA* **97**, 7561–7566 (2000).
9. Smith, D. S. & Tsai, L. H. Cdk5 behind the wheel: a role in trafficking and transport? *Trends Cell Biol.* **12**, 28–36 (2002).
10. Tu, Y., Tornaletti, S. & Pfeifer, G. P. DNA repair domains within a human gene: selective repair of sequences near the transcription initiation site. *EMBO J.* **15**, 675–683 (1996).
11. Tchou, J. *et al.* Substrate specificity of Fpg protein. Recognition and cleavage of oxidatively damaged DNA. *J. Biol. Chem.* **269**, 15318–15324 (1994).
12. Lindahl, T. & Barnes, D. E. Repair of endogenous DNA damage. *Cold Spring Harb. Symp. Quant. Biol.* **65**, 127–133 (2000).
13. Bruner, S. D., Norman, D. P., Fromme, J. C. & Verdine, G. L. Structural and mechanistic studies on repair of 8-oxoguanine in mammalian cells. *Cold Spring Harb. Symp. Quant. Biol.* **65**, 103–111 (2000).
14. Athas, W. F., Hedayati, M. A., Matanoski, G. M., Farmer, E. R. & Grossman, L. Development and field-test validation of an assay for DNA repair in circulating human lymphocytes. *Cancer Res.* **51**, 5786–5793 (1991).
15. Landfield, P. W. & Pitler, T. A. Prolonged Ca²⁺-dependent afterhyperpolarizations in hippocampal neurons of aged rats. *Science* **226**, 1089–1092 (1984).
16. Longo, V. D. & Finch, C. E. Evolutionary medicine: from dwarf model to healthy centenarians? *Science* **299**, 1342–1346 (2003).
17. Hekimi, S. & Guarente, L. Genetics and specificity of the aging process. *Science* **299**, 1346–1351 (2003).
18. Hasty, P., Campisi, J., Hoejmackers, J., van Steeg, H. & Vijg, J. Aging and genome maintenance: lessons from the mouse? *Science* **299**, 1355–1359 (2003).
19. Murphy, C. T. *et al.* Genes that act downstream of DAF-16 to influence the lifespan of *Caenorhabditis elegans*. *Nature* **424**, 277–283 (2003).
20. Ghosh, R. & Mitchell, D. L. Effect of oxidative DNA damage in promoter elements on transcription factor binding. *Nucleic Acids Res.* **27**, 3213–3218 (1999).
21. Kyng, K. J., May, A., Kolvrå, S. & Bohr, V. A. Gene expression profiling in Werner syndrome closely resembles that of normal aging. *Proc. Natl Acad. Sci. USA* **100**, 12259–12265 (2003).
22. Mecocci, P. *et al.* Oxidative damage to mitochondrial DNA shows marked age dependent increases in human brain. *Ann. Neurol.* **34**, 609–616 (1993).
23. McCarroll, S. A. *et al.* Comparing genomic expression patterns across species identifies shared transcriptional profile in aging. *Nature Genet.* **36**, 197–204 (2004).

24. Tusher, V. G., Tibshirani, R. & Chu, G. Significance analysis of microarrays applied to the ionizing radiation response. *Proc. Natl Acad. Sci. USA* **98**, 5116–5121 (2001).
25. Xu, J. *et al.* Dopamine-dependent neurotoxicity of alpha-synuclein: A mechanism for selective neurodegeneration in Parkinson disease. *Nature Med.* **8**, 600–606 (2002).

Supplementary Information accompanies the paper on www.nature.com/nature.

Acknowledgements We thank G. Verdine and D. Gabuzda for discussions, and M. Yuan, S. Weninger, P. Stieg, P. Dicks, C. Geula and L.-W. Jin for assistance with procurement and dissection of tissue samples. We also acknowledge the Kathleen Price Bryan Brain Bank at Duke University, the Harvard Brain Tissue Resource Center, the Massachusetts General Hospital ADRC Brain Bank, the University of Washington Brain Bank, and the University of Maryland Brain Bank for providing tissue samples. This work was supported in part by grants from the NIH (NIA and NINDS) to B.A.Y. T.L. was supported by a fellowship from the National Institute on Aging, and S.Y.K. was supported by a fellowship from the Leukemia and Lymphoma Society.

Competing interests statement The authors declare that they have no competing financial interests.

Correspondence and requests for materials should be addressed to B.A.Y. (Bruce.Yankner@childrens.harvard.edu).

.....

Mismatch repair genes identified using genetic screens in Blm-deficient embryonic stem cells

Ge Guo, Wei Wang & Allan Bradley

The Wellcome Trust Sanger Institute, Hinxton, Cambridge CB10 1SA, UK

Phenotype-driven recessive genetic screens in diploid organisms require a strategy to render the mutation homozygous. Although homozygous mutant mice can be generated by breeding, a reliable method to make homozygous mutations in cultured cells has not been available, limiting recessive screens in culture. Cultured embryonic stem (ES) cells¹ provide access to all of the genes required to elaborate the fundamental components and physiological systems of a mammalian cell. Here we have exploited the high rate of mitotic recombination in Bloom’s syndrome protein (Blm)-deficient ES² cells to generate a genome-wide library of homozygous mutant cells from heterozygous mutations induced with a revertible gene trap³ retrovirus. We have screened this library for cells with defects in DNA mismatch repair (MMR), a system that detects and repairs base–base mismatches⁴. We demonstrate the recovery of cells with homozygous mutations in known and novel MMR genes. We identified *Dnmt1*(ref. 5) as a novel MMR gene and confirmed that *Dnmt1*-deficient ES cells exhibit micro-satellite instability⁶, providing a mechanistic explanation for the role of *Dnmt1* in cancer. The combination of insertional mutagenesis in Blm-deficient ES cells establishes a new approach for phenotype-based recessive genetic screens in ES cells.

In order to establish a genetic background in which homozygous mutations could be readily recovered, we generated mice and ES cells with double-targeted mutations in the *Blm* locus^{2,7}. We have previously established that Blm-deficient cells carrying heterozygous mutations segregate homozygous daughters *in vitro* and *in vivo*, presumably through mitotic recombination between non-sister chromatids^{2,8} (Fig. 1a). The rate of loss of heterozygosity (LOH), determined by Luria–Delbruck fluctuation analysis, is 4.2×10^{-4} events per locus per cell per generation in Blm-deficient ES cells, which is elevated 18-fold compared with wild type cells². In practical terms, a single Blm-deficient ES cell with a heterozygous autosomal mutation will have segregated several